Biochimica et Biophysica Acta 1848 (2015) 1352–1358

Contents lists available at ScienceDirect

Biochimica et Biophysica Acta

journal homepage: www.elsevier.com/locate/bbamem

Cationic amphipathic peptides KT2 and RT2 are taken up into bacterial cells and kill planktonic and biofilm bacteria

Thitiporn Anunthawan [a,b], César de la Fuente-Núñez [c], Robert E.W. Hancock [c,*], Sompong Klaynongsruang [a,b,**]

[a] Department of Biochemistry, Faculty of Science, Khon Kaen University, Khon Kaen, Thailand
[b] Protein and Proteomics Research Center for Commercial and Industrial Purposes (ProCCI), Khon Kaen University, Khon Kaen, 40002, Thailand
[c] Department of Microbiology and Immunology, Centre for Microbial Diseases and Immunity Research, 232–2259 Lower Mall Research Station, University of British Columbia, Vancouver, BC V6T 1Z4, Canada

ARTICLE INFO

Article history:
Received 20 September 2014
Received in revised form 19 February 2015
Accepted 20 February 2015
Available online 10 March 2015

Keywords:
Antibacterial mechanism
DNA binding
Antibiofilm peptide
Antibacterial peptide
RT2
KT2

ABSTRACT

We investigated the mechanisms of two tryptophan-rich antibacterial peptides (KT2 and RT2) obtained in a previous optimization screen for increased killing of both Gram-negative and Gram-positive bacteria pathogens. At their minimal inhibitory concentrations (MICs), these peptides completely killed cells of multidrug-resistant, enterohemorrhagic pathogen *Escherichia coli* O157:H7 within 1–5 min. In addition, both peptides exhibited anti-biofilm activity at sub-MIC levels. Indeed, these peptides prevented biofilm formation and triggered killing of cells in mature *E. coli* O157:H7 biofilms at 1 μM. Both peptides bound to bacterial surface LPS as assessed using the dansyl-polymyxin displacement assay, and were able to interact with the lipids of liposomes as determined by observing a tryptophan blue shift. Interestingly, even though these peptides were highly antimicrobial, they did not induce pore formation or aggregates in bacterial cell membranes. Instead these peptides readily penetrated into bacterial cells as determined by confocal microscopy of labeled peptides. DNA binding assays indicated that both peptides bound to DNA with higher affinity than the positive control peptide buforin II. We propose that cationic peptides KT2 and RT2 bind to negatively-charged LPS to enable self-promoted uptake and, subsequently interact with cytoplasmic membrane phospholipids through their hydrophobic domains enabling translocation across the bacterial membrane and entry into cells within minutes and binding to DNA and other cytoplasmic membrane. Due to their dual antimicrobial and anti-biofilm activities, these peptides may find use as an alternative to (or in conjunction with) conventional antibiotics to treat acute infections caused by planktonic bacteria and chronic, biofilm-related infections.

1. Introduction

Bacterial drug resistance is a major problem in human health as it has led to the reduced efficacy of conventional antibiotics. Thus, the identification of novel antibiotic compounds is essential. Antimicrobial peptides have been proposed as a promising alternative to conventional antibiotics in part due to their potency at low concentrations and to the fact that they are less prone to select for antimicrobial resistance [1–4]. Certain peptide antibiotics that exhibit potent antimicrobial properties have been designed and synthesized based on their biochemical and biophysical properties. However, the relationship between these properties and antibacterial activity is unclear. Two main types of antibacterial mechanisms have been reported involving the bacterial membrane as a target and diverse intracellular targets, and it has been further suggested that peptides can have complex mechanisms involving multiple targets [1–4]. Membrane targeting has been proposed to involve the loss of cellular integrity as a result of perforation of membranes and diverse hypotheses have been used to explain this including the barrel stave channel, torroidal pore, carpet and aggregate models [1–3]. For example, the antibacterial mechanisms of magainin II [5], alamethicin [6] and polymyxin B [7] have been reported to involve torroidal pores, barrel stave channels and carpet mechanism respectively. Many antibacterial peptides have been reported to translocate across the cytoplasmic membrane to access intracellular targets [2,3], including e.g. buforin II (binds to DNA) [8] and PR-39 (inhibits DNA/RNA/protein synthesis) [9].

Here we characterized the mechanism of action of two antimicrobial peptides KT2 (NGVQPKYKWWKWWKKWW-NH_2) and RT2 (NGVQPKYRWWRWWRRWW-NH_2) that differ only by 4 K → R substitutions. These peptides were previously found to have good antibacterial activity against *Escherichia coli* and *Salmonella typhi* but to be non-toxic against human red blood cells, Vero kidney epithelial cells from African green monkey and RAW 264.7 mouse macrophage cells [10]. Both peptides are disordered in buffer but substantially α-helical

* Corresponding author. Tel.: +1 604 822 2682; fax: +1 604 827 5566.
** Correspondence to: S. Klaynongsruang, Department of Biochemistry, Faculty of Science, Khon Kaen University, Khon Kaen, Thailand. Tel./fax: +66 43 342911.
E-mail addresses: bob@hancocklab.com (R.E.W. Hancock), somkly@kku.ac.th (S. Klaynongsruang).

http://dx.doi.org/10.1016/j.bbamem.2015.02.021
0005-2736/

in lipid membranes. However despite interacting well with membranes and membrane mimetics, the work here suggested that they act intracellularly rather than by damaging membranes.

2. Materials and methods

2.1. Chemical and reagents

1,2-Dioleoyl-*sn*-glycero-3-phosphocholine (DOPC), 1,2-dioleoyl-*sn*-glycero-3-phospho-rac-(1-glycerol) (DOPG) and a miniextruder for making liposomes from these lipids were obtained from Avanti Polar Lipids, Inc. (Alabaster, AL, USA). 8-aminonaphthalene-1,3,6 trisulfonic acid (ANTS)/p-xylene-bis-pyridinium bromide (DPX) and Vybrant Dil cell-labeling solution were gained from Invitrogen (Oregon, USA). Dansyl-polymyxin was synthesized by Evan F. Haney. LPS from *Escherichia coli* 0111:B4 which was purified by phenol extraction was purchased from Sigma-Aldrich (USA). *EcoR*1 digested DNA was obtained from Promega US G1721, Madison, WI, USA.

2.2. Peptide synthesis

Peptides and FITC (fluorescein isothiocyanate) labeled peptides at N terminal were synthesized by standard Fmoc solid phase chemistry at GL Biochem (Shanghai, China) and purified to ≥95% purity using (RP)-HPLC (stationary phase: C-18, mobile phase: varying from 5% to 20% acetonitrile in water, 0–20 min). The exact molecular weight of each peptide was confirmed via MALDI-TOF MS.

2.3. Killing kinetic

E. coli O157:H7 cells were inoculated in LB broth in mid-log phase (OD_{600} = 0.5–0.6) and then the suspension was diluted in 1× BM2 salt to an OD_{600} equivalent of 0.001 (~1×10^6 CFU/ml). Subsequently cells were treated with peptides at concentrations corresponding to their MIC against *E. coli*. The percentage of bacterial survival was subsequently monitored at time points 0, 1, 5, 10, 60 min by assessing colony forming units after plating on LB agar plates overnight [11]. Percent survival was calculated as $(T_{60}/T_0) \times 100$, where T_{60} and T_0 represented the colony forming units at 60 min and at the time before adding the peptides respectively.

2.4. Biofilm flow cell assays

E. coli O157:H7 biofilms were grown as previously described [12] for 72 h in BM2 minimal glucose medium [62 mM potassium phosphate buffer, pH 7.0, 7 mM $(NH_4)_2SO_4$, 2 mM $MgSO_4$, 10 μM $FeSO_4$, containing 0.4% (wt/vol) glucose as a carbon source] at 37 °C in flow cell chambers with channel dimensions of 1 × 4 × 40 mm in the absence or presence of 1 μM KT2 and RT2 in the flow-through medium. Biofilm cells were stained using the Live/Dead BacLight bacterial viability kit (Molecular Probes, Eugene, OR) prior to confocal microscopy performed using a confocal laser scanning microscope (Olympus, Fluoview FV1000). Three-dimensional reconstructions of the resultant biofilms were generated by using the Imaris software package (Bitplane AG).

2.5. LPS binding

Binding of peptides to *E. coli* 0111:B4 LPS was assessed using the dansyl-polymyxin displacement assay as previously described [13]. The I_{50} was the concentration that decreased the maximal fluorescence of bound dansyl polymyxin by 50%.

2.6. Aggregation

The aggregation assay was performed as previously described [14]. Briefly, large unilamellar vesicles (LUV/liposomes) were prepared by dissolving phospholipids (DOPG and DOPC at a weight ratio of 2:3) in chloroform, and then evaporating overnight to obtain lipid films. The lipid films were then hydrated by the addition of 10 mM Tris–HCl buffer and shaking to obtain multilamellar vesicles. After 5 freeze-thaw cycles in CO_2, the vesicles were extruded 20 times through a miniextruder with a 0.2 mm polycarbonate membrane to make LUV. The ability of antibacterial peptides to trigger LUV aggregation was determined by using a microplate reader to monitor the absorbance at 415 nm after incubation with peptides for 15 min at peptide to lipid molar ratios of 1:1–1:20. The absorbance of LUVs suspended in 20 mM Tris–HCl was subtracted as the background from the absorbance of LUV in the presence of peptides.

2.7. Membrane leakage

LUVs were prepared as above except lipid films were hydrated by adding 10 mM Tris–HCl buffer, pH 7.4, which contains 12.5 mM ANTS fluorophore, 45 mM DPX quencher, 20 mM NaCl [15]. The free dye and quencher were removed from the resultant LUVs by using gel filtration chromatography on Sephadex G 25. The liposome concentration was tested by calorimetry [16]. Dynamic light scattering was used to measure the liposome size which was 0.135 μm. The peptides were added into the liposome suspension at a peptide to lipid molar ratio of 1:1 to 1:100. The peptides caused release of ANTS as well as the quencher DPX which when diluted into the extra-liposome volume dissociated leading to an increase in ANTS fluorescence. Therefore, after incubation for 60 min, the ANTS fluorescence intensity was measured using a SpectraMax M5 microplate reader (Molecular Devices) at an excitation wavelength of 386 nm and emission wavelength of 512 nm. The percentage of small molecular ANTS leakage was calculated as the following formula $(F_s - F_n)100/F_P - F_n$ where F_s, F_n and F_P represent the fluorescence intensity of the peptide-treated liposome suspension, negative control (liposome suspension without peptide) and 2% Triton × 100-treated liposomes (100% leakage control), respectively. The Fs values were corrected by subtracting the background fluorescence of peptide in buffer.

2.8. Interaction with membranes: tryptophan blue shift

The entry of tryptophan in a peptide into a hydrophobic environment such as a membrane, leads to an increase in fluorescence and a blue shift as the tryptophan head group has increased mobility. A previously reported method [17] was adapted whereby the change in the maximum emission spectrum of tryptophan amino acids of AMPs (Antimicrobial peptides) upon interaction with LUV mimicking the bacterial membrane was determined by using a Multifunction Microplate Reader (Thermo Fisher, Finland). Liposomes and peptides were mixed in 20 mM Tris–HCl at molar ratios ranging from 1:1 to 1:20. After excitation at 280 nm, emission spectra were recorded from 300 to 400 nm at a scan rate of 60 nm/min. The spectra of the liposome-only background was subtracted from that of peptides in the presence of liposomes (0.2 mM) and compared with the peak emission wavelength of peptide alone in buffer at the same concentrations.

2.9. DNA binding assay

The binding of peptides to DNA was examined by a gel retardation assay as described by Park et al. [8]. *EcoRI*-treated DNA was used and mixed with 10× binding buffer comprised of 100 mM Tris–HCl, 200 mM KCl, 10 mM EDTA, 10 mM DTT and 50% (v/v) glycerol, water and peptides at increasing peptide to DNA ratios of 0:1, 0.5:1, 1:1, 2:1, 4:1 and 8:1. Magainin II and buforin II were used as negative and positive controls respectively. After incubation for 1 h at 25 °C, 2 μl of loading buffer was mixed and loaded on a 0.75% agarose/TAE gel and run at 108 V and 70 mA for 1.5 h after which the gel was stained with ethidium bromide.

2.10. Translocation assays: bacterial cells

Bacterial cells were grown to mid-log phase and then diluted to a final OD_{600} of 0.001. The cells were washed 3 times with phosphate buffered saline (PBS) and resuspended in PBS. Subsequently, the fluorescein isothiocyanate (FITC)-labeled peptides (at 0.5× and 2× MIC) were incubated for 60 min after which the treated bacterial cells were centrifuged at 5000 rpm for 15 min. The pellet was collected and washed 3 times and then resuspended in PBS. The location of FITC-labeled peptides was then visualized using confocal microscopy at an excitation wavelength of 490 nm and an emission wavelength of 525 nm.

2.11. Translocation assays: GUVs

Giant unilamellar vesicles (GUVs) were prepared as outlined previously [18,19]. Briefly, phospholipids (3DOPC: 2DOPG weight ratio) were dissolved in chloroform, and 1 μl of Vybrant Dil then lipid films were obtained by evaporating the solvent under a stream of N_2 and then subjecting the film to high vacuum for at least 2 h. The lipid films were pre hydrated with steam and then hydrated by gently adding 200 μl of 250 mM saccharose. After incubation for at least 60 min, a GUV suspension of approximately 2.5 mM lipids was obtained. The FITC-labeled peptides and Vybrant Dil dye labeled GUVs were mixed together at a 1:1 peptide to lipid molar ratio. The location of FITC-labeled peptides was then detected by using confocal microscopy at an excitation wavelength of 549 nm and an emission wavelength of 565 nm.

3. Results and discussion

3.1. Time kill assay

Most AMPs kill very rapidly. KT2 and RT2 were able to kill *E. coli* O157:H7 at concentrations of 5 μM/11 μg/ml and 18 μM/46 μg/ml (the MICs of KT2 and RT2 respectively, against *E. coli* within 1 min and 5 min, respectively). Cell killing at lower concentrations clearly indicated that the antibacterial mechanism of these peptides was concentration-dependent (Fig. 1A and B). These results extended previous studies using scanning electron microscopy in which perturbation of *E. coli* ATCC 25922 was detected within 1 min of incubation at 10-fold higher concentrations of peptides [10].

3.2. Anti-biofilm activity

Flow cell methodology was used to assess the anti-biofilm properties of peptides KT2 and RT2. *E. coli* O157:H7 biofilms were grown for 3 days in flow cell chambers and were left untreated or were treated with 1 μM of each peptide (i.e. well below the planktonic MIC) starting at either day 0 (inhibition conditions) or day 2 (eradication conditions) (Fig. 2). When added to the flow-through medium at the beginning of biofilm growth on day 0, both peptides completely prevented biofilm development at concentrations far below their MIC (Fig. 2, upper right panels). Both peptides substantially induced killing of cells present in pre-existing biofilms (i.e. when peptides were first added after 2 days of biofilm growth) (Fig. 2, bottom panels).

3.3. LPS binding

The initial interaction of cationic peptides with Gram negative bacteria involves self promoted uptake across the outer membrane whereby the peptides bind to anionic LPS on the surface and cause perturbation of outer membrane structure to promote their own passage across the membrane [13]. Since both peptides RT2 and KT2 showed antibacterial activity against *E. coli* and characteristic cell blebbing in scanning electron micrographs [10], we tested here their ability to bind to LPS, a major membrane component of Gram-negative bacteria using the

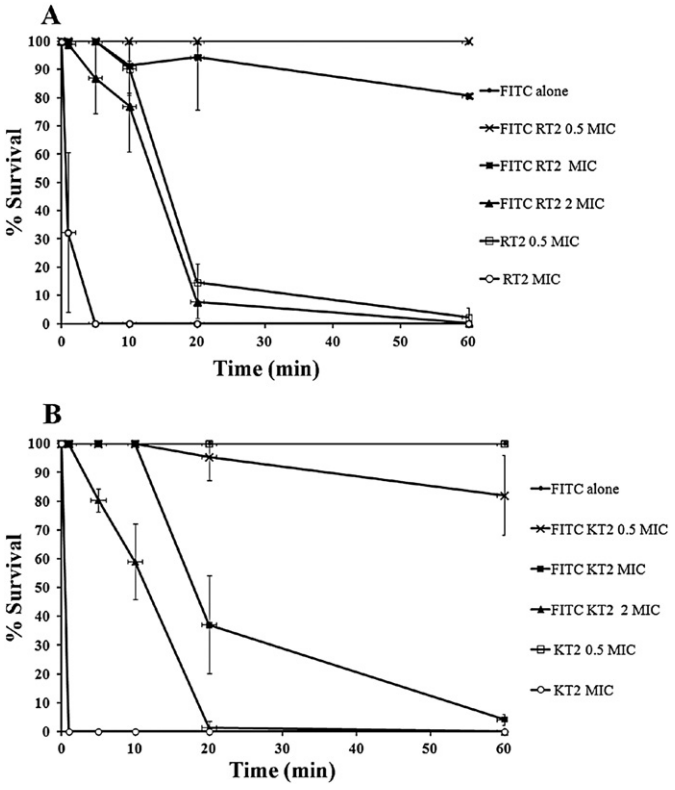

Fig. 1. Killing kinetics. (A) Time-kill study of *E. coli* O157:H7 exposed to different concentrations of peptide RT2. The experiment was performed three times. (B) Killing curve of *E. coli* O157:H7 exposed to KT2 at various concentrations relative to the MIC. The experiment was performed three times.

DPX displacement assay. Peptides KT2 and RT2 were able to displace dansyl-polymyxin effectively with I_{50} of 4.6 and 5.8 μM respectively whereas polymyxin B, which was used as a positive control [20] had an I_{50} of 0.76 μM (Fig. 3). These data are consistent with both peptides being able to initially interact with the outer membrane at divalent cation binding sites on LPS, indicating transposition across the outer membrane by self-promoted uptake [11,13].

3.4. Aggregation of lipids

Lipid aggregation has been proposed to be involved in the killing bacteria by certain AMPs, consistent with the carpet [15], torroidal pore [5], and aggregate [13] models. Polymyxin B and magainin II were used as positive controls as their mechanisms of action have been proposed to involve membrane disruption [4,5]. Polymyxin B exhibited a strong ability to induce liposome aggregation (Fig. 4) while magainin II was quite weak (Fig. 4). In contrast, buforin II, which acts through an intracellular target [8], as well as RT2 and KT2, were unable to trigger liposome aggregation even at lipid peptide molar ratios of 1:1 (Fig. 4).

3.5. Membrane leakage

The ability of peptides to cause perforation of liposomes as assessed by leakage of small molecules has been used to determine whether peptides can disrupt membranes. Most cationic peptides will do this at effective peptide to lipid ratios, but many only cause liposome perforation at high peptide to lipid ratios. Magainin II was able to make pores on bacterial-membrane mimicking liposomes resulting in the membrane leakage of almost 100% at peptide-to-lipid molar ratios of 1:5 and 1:10 as shown previously [5]. Buforin II showed a substantially decreased ability to induce pore formation in liposomes [21], when

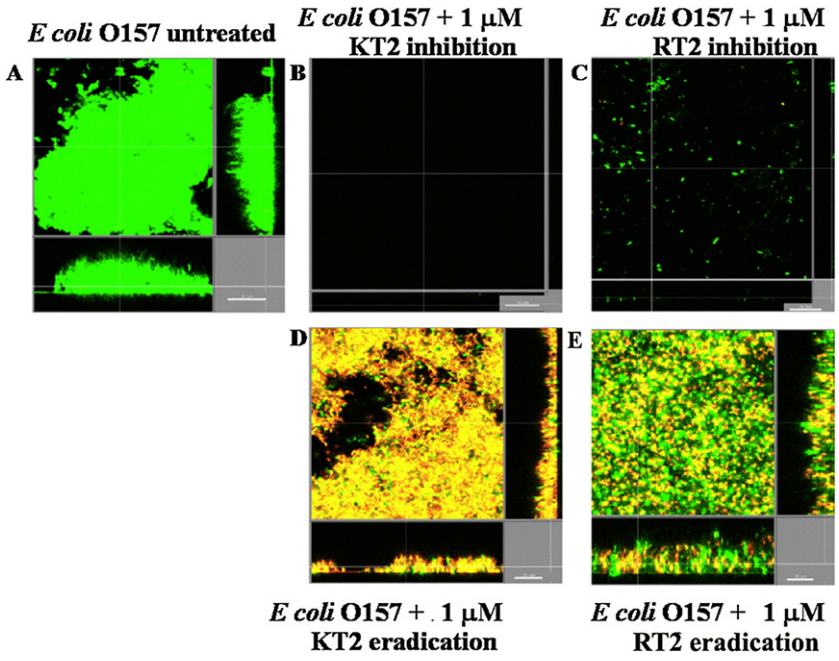

Fig. 2. Peptides KT2 and RT2 prevented biofilm formation and killed cells within pre-formed *E. coli* O157 biofilms. Sub-lethal concentrations (1 μM) of peptides KT2 and RT2 were used. Inhibition of biofilm development was tested by adding peptide at day 0 into the flow-through medium of the flow cell apparatus and then monitoring biofilm formation for a total of 3 days as can be seen in panels (B) (KT2) and (C) (RT2). Eradication conditions involved allowing biofilms to grow for 2 days to reach their mature state before addition of either peptide into the flow-through medium. (A) is a negative control that is a 3-day-old biofilm without peptide treatment; (D) and (E) are 0-day-old biofilms treated with KT2 and RT2 respectively. After 3 days, bacteria attached to the surface of flow cells were stained green with the bacteria stain Syto-9 and red with the dead-bacteria stain propidium iodide (merge shows as yellow to red) prior to confocal imaging. Each panel shows reconstructions from the top in the large panel and sides in the right and bottom panels (xy, yz and xz dimensions).

compared to magainin II (Fig. 5). Indeed, buforin II-treated liposomes showed less than 50% leakage at the highest peptide to lipid molar ratio (1:5) (Fig. 5). On the other hand, polymyxin B, RT2 and KT2 were unable to induce leakage of small molecules at all concentrations tested (Fig. 5). Thus it seemed unlikely that our peptides worked by busting membranes.

3.6. Interaction with membrane lipids

Since both RT2 and KT2 have tryptophan residues, we could use this to assess the ability of these peptides to interact with and insert into the lipid core of LUV since a hydrophobic environment causes an increase in fluorescence and a blue fluorescence emission maximum at an excitation wavelength of 280 nm. Both peptides interacted with the hydrophobic cores of membranes at peptide-to-lipid molar ratios of 1:10 as can be seen in Table 1, consistent with the prior observation of increased α-helicity after interaction with liposomes [22]. KT2 which has greater hydrophobicity could potentially bury deeper in lipid bilayer than RT2, due to hydrophobic interactions between peptides and lipid core. The ability to bury deeper in lipid bilayers however would not imply better translocation of a peptide [23,24]. Indeed peptides with higher hydrophobicity might have weaker penetrating ability since peptides interact more strongly with the lipid core of the liposome [25]. This result taken together with the lack of membrane leakage indicates that the peptides might interact with membranes in the process of translocation across the bilayer.

3.7. Translocation into bacterial cells

To enable direct visualization of whether these peptides could penetrate bacterial cells, peptides were labeled with FITC labeling. To control for any effects of labeling on peptide activity, killing curve assays were conducted. FITC labeling of these peptides reduced the antibacterial activity of the peptides compared to their non-FITC labeled variants (Fig. 1A and B). Indeed, FITC-RT2 at 2× MIC of RT2 killed all bacterial cells only after 60 min, whereas RT2 at its MIC killed all cells within 5 min (Fig. 1A). Similarly, FITC-labeled KT2 at 2× MIC of KT2 killed the entire *E. coli* O157:H7 population within 20 min, whereas KT2 at its MIC eradicated all bacteria within 1 min (Fig. 1B). Moreover, a negative control with FITC alone at a final concentration of 24 mM showed no antibacterial activity in any experiments (Fig. 1A and B). Subsequent

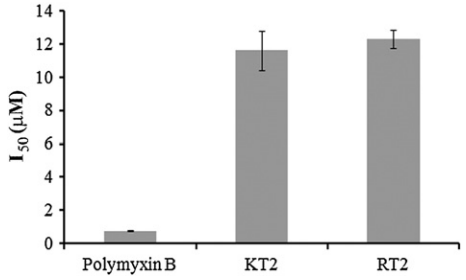

Fig. 3. LPS binding activity assessed as the I_{50} of dansyl-polymyxin displacement from *Escherichia coli* 0111:B4 LPS. Each value is averaged from three experiments ± the standard deviation.

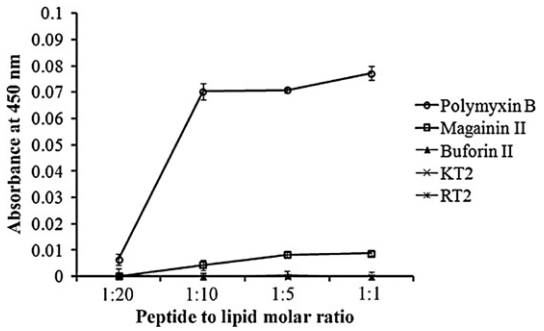

Fig. 4. Liposome aggregation assays. Liposome aggregation was assessed by the increase in A_{450} after the addition to LUV of designed peptides and control peptides polymyxin B, magainin II and buforin II.

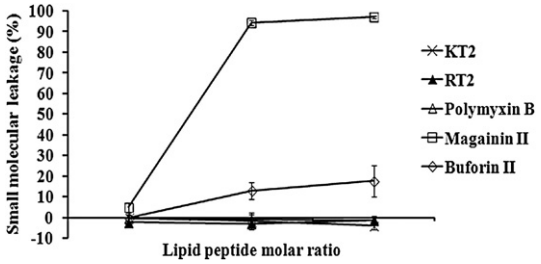

Fig. 5. Liposome leakage assays. Leakage of probe molecules from liposomes induced by treatment with KT2 and RT2 compared to control peptides polymyxin B, magainin II and buforin II.

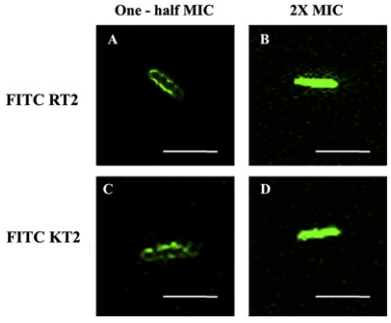

Fig. 6. Translocation studies using live bacterial cells. Translocation of FITC-labeled RT2 and KT2 into bacterial cells (*E. coli* O157) was visualized by using confocal microscopy. Panels (A) and (C) correspond to one-half MIC of RT2 and KT2, respectively. Panels (B) and (D) correspond to 2 × MIC of RT2 and KT2 respectively. The white line in each panel is equivalent to 5 μm. At 2 × MIC of both peptides, an image corresponding to the rigid rod of bacterial cells was found in all stacks of confocal images while an image corresponding to the outline of bacterial cells was found in some stacks at one-half MIC of both peptides.

translocation studies with the labeled peptides used 2 × MIC of peptides to adjust for this lower antibacterial activity. The labeling of peptides with fluorescent tags can change their biochemical and biophysical properties and this decrease the killing ability of peptides as observed here and previously [26]. The lower activity of our FITC labeled peptides was likely due to the reduction in the positive charge due to the covalent bond formed between the N terminal amine and FITC.

To assess whether the peptides could penetrate into *E. coli* O157:H7 cells or remained membrane associated, we used confocal microscopy after interacting peptides with cells. At 0.5× MIC, both FITC-labeled peptides primarily bound to the bacterial membrane and did not penetrate into bacterial cells (Fig. 6A and C). These results correlated with the kill curve assays, in which neither FITC-RT2 (Fig. 1A) nor FITC-KT2 (Fig. 1B) led to substantial bacterial cell killing at these concentrations. However, at concentrations corresponding to 2× MIC, both FITC-labeled peptides penetrated rapidly into bacterial cells without disrupting them and were observed as filled green rods in all confocal sections through the cells (Fig. 6B and D). These results correlated with killing curves using both these fluorescently-labeled peptides at 2× MIC, which indicated complete cell killing within 60 min (Fig. 1A and B). CPPs are cationic (often amphipathic) peptides that can cross the cell membrane via energy-independent and/or energy-dependent mechanisms [27–31]. Many previous studies report that CPPs in which Lys is replaced with Arg can more efficiently cross membranes, although these studies were generally performed in eukaryotic cells or model systems with weak electrical potential gradients [31]. However, in this study involving bacterial uptake into bacterial cells with substantial electrical potential gradients, differences in the cell penetrating ability of RT2 and KT2 were not clear since green rods were observed in all stacks of cells treated with RT2 and KT2.

3.8. Interaction with GUVs

To study the interaction of peptides KT2 and RT2 with another membrane lipid system, we used giant unilamellar vesicles (GUVs) as an experimental model to mimic bacterial membranes, and visualized interactions using confocal microscopy. In the absence of peptide, we observed hollow rigid circles stained red with the Vybrant Dil dye and correspond to the membranes of the GUVs (Fig. 7). FITC alone, used as a negative control at a final concentration of 1.3 mM, did not penetrate into the GUVs (Fig. 7). Similarly, for FITC-RT2 and FITC-KT2, there were no green peptide spots in the GUVs as can be seen in the micrographs and the fluorescent intensity graphs of Fig. 7, thus indicating that they likely preferentially buried into the bacterial membrane as opposed to crossing the bilayer into the interior of GUVs. The intact shapes of peptide-treated GUVs (Fig. 7) suggested that these peptides did not destroy the bacterial membrane-like GUVs. Moreover, the differential roles of Arg and Lys in RT2 and KT2 respectively in interacting with bacterial membrane mimics was not clear in this study, since they seemed to have similar activity in penetrating liposomes. The inability of peptides to penetrate well into the interior of GUVs (Fig. 7) contrasts with their ability to readily cross the membrane of live bacterial cells (Fig. 6). This is likely due to the electrical potential gradient across the cytoplasmic membrane of bacterial cells (around −130 mV providing a force for the inwards movement of cationic peptides) combined with the presence of negatively-charged intracellular DNA that might trap the translocated peptides. The reason for this may be the translocation ability of them depends on the force of electrostatic interaction of lipid core-burying peptides and negatively charge components. It should be pointed out that in making GUVs we used PC, which is compatible as a surrogate for PE, the major phospholipid in the *E. coli* membrane. Although, other studies have shown that PE is usually freely interchangeable with PC and other neutral lipids in liposome studies it is possible that the different shape of PC also interfered with translocation.

Table 1
Interaction of peptide tryptophan residues with the hydrophobic core of liposomes. This was assessed as the blue shift in tryptophan maximum emission wavelengths (nm) of KT2 and RT2 in LUV composed of zwitterionic (DOPC) and anionic (DOPG) phospholipids.

Peptide	Tryptophan blue shift (nm)		
	1:1 (P/L)	1:5 (P/L)	1:10 (P/L)
KT2	10 nm	4 nm	4 nm
RT2	6 nm	2 nm	ND

ND indicates not determined since the fluorescence intensity of peptides in buffer could not be detected.

3.9. DNA binding

The experiments described above, indicate that it is unlikely that membrane targeting is the mechanism of action of peptides RT2 and KT2. Therefore, these peptides were tested for their ability to bind to intracellular DNA (Fig. 8), since the electrostatic interactions between the positive charges of the peptides, which are burying in the lipid core (Table 1), and the negative charge of DNA might lead the peptides to accumulate within bacterial cells and also provide a potential mechanism of action [3]. Magainin II, which has poor DNA-binding ability [8,32], was used as a negative control (Fig. 8). Indeed, magainin II did not bind to DNA at any of the ratios tested, in accordance with a previous study [8]. Both peptides RT2 and KT2 bound avidly to DNA (Fig. 6). Peptide KT2 had the strongest ability to bind to DNA at a 1:1 DNA:peptide weight ratio, which was substantially higher than that previously reported for buforin II (1:10 DNA: peptide weight ratio) [8]. The DNA retardation of peptide RT2 was visualized at a 1:2 DNA:peptide ratio, which also represented increased binding compared to buforin II (Fig. 8). These results are consistent with the conclusion that the antibacterial action of peptides KT2 and RT2 might involve DNA binding. Moreover, comparing the % helical content of RT2 and KT2 in the

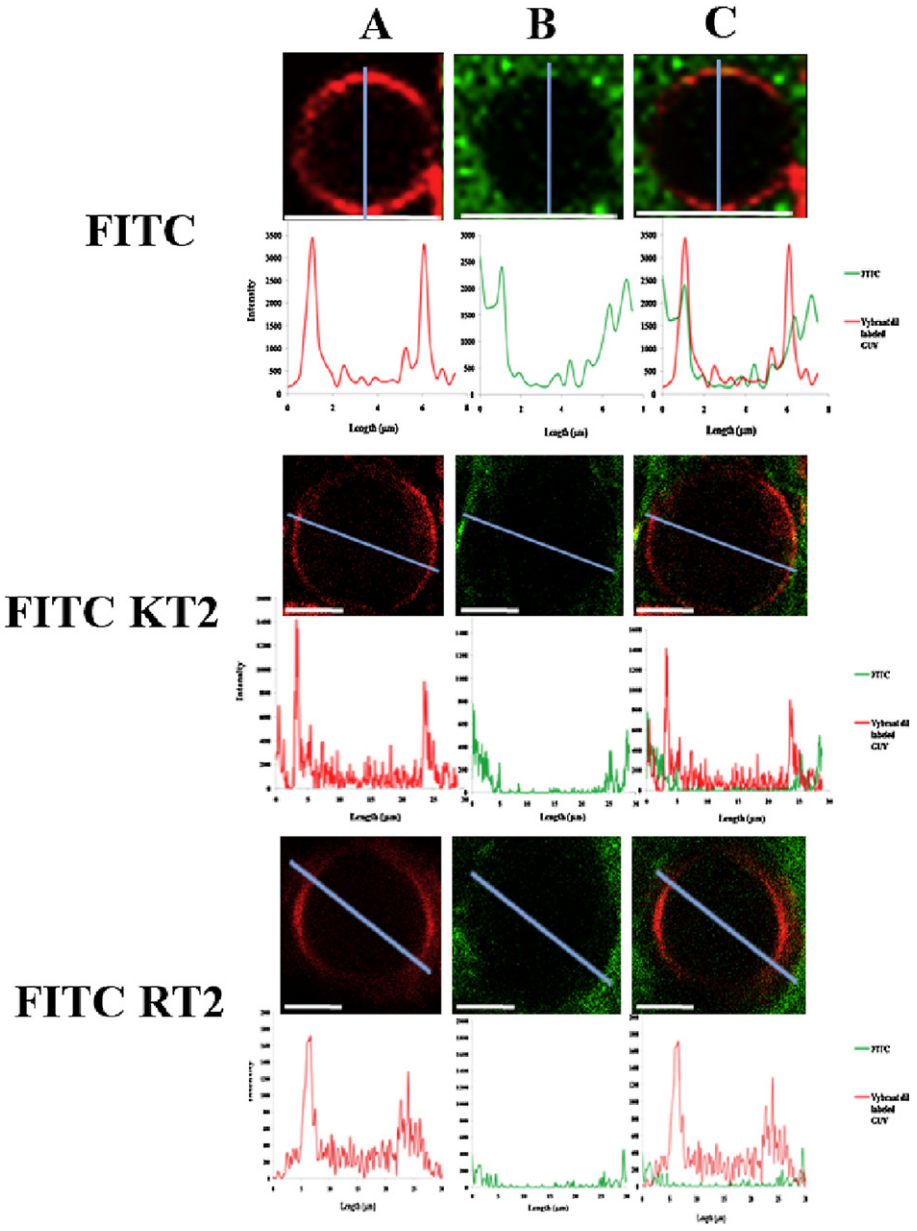

Fig. 7. Translocation studies using giant unilamellar vesicles (GUVs). Translocation of FITC-labeled peptides RT2 and KT2 into GUVs. GUVs, which were composed of bacteria-like lipids, were visualized by using confocal microscopy. The panels in column (A) show the morphologies of GUVs where the red fluorescence of Vybrant Dil dye was used to label GUVs. The panels in column (B) indicated the locations of green FITC-labeled peptides and FITC alone (negative control). The panels in column (C) show the merged images of the corresponding images in columns (A) and (B). The white line in each panel is equivalent to 10 μm. The fluorescent intensity in the corresponding area (the blue line) is shown at the bottom of each panel.

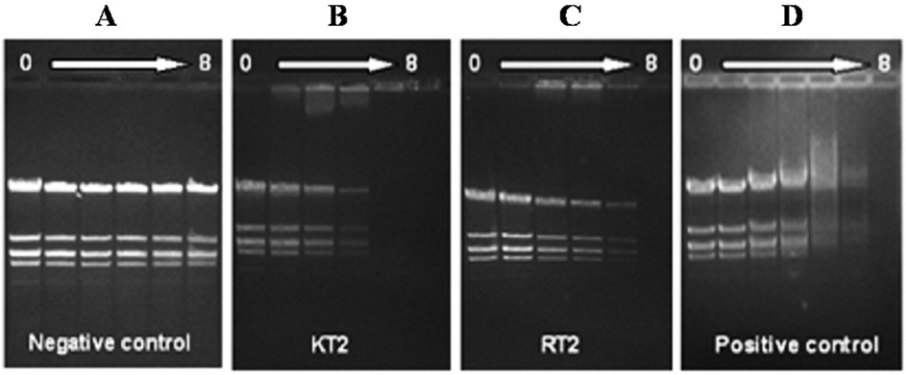

Fig. 8. DNA binding. Peptide binding to DNA as assessed by banding pattern on a 0.75% agarose/TAE gel at different peptide:plasmid weight ratios. The peptide-to-DNA weight ratios were 0:1, 0.5:1, 1:1, 2:1, 4:1 and 8:1, respectively, from left to right. '0' in the first lane indicates the negative control (no peptide addition). (A), (B), (C) and (D) are results for magainin II (negative control peptide), RT2, KT2, and buforin II (positive control peptide), respectively.

environment of bacterial membrane mimics and in buffer as can be seen in the previous studies [10], the helical content of these peptides seems not important for their antibacterial mechanism, which is the same as buforin II, while the helical content is a distinct characteristics of membrane active peptides such as magainin II [32].

4. Conclusions

This study indicates that the antibacterial mechanisms of peptides KT2 and RT2 are similar and likely result in uptake across the outer and cytoplasmic membrane of bacteria leading to DNA binding. The positively charged peptides were able to interact strongly with negatively charged bacterial surface LPS, by using both electrostatic as well as hydrophobic interactions. This would lead to self-promoted uptake and consequent translocation of the peptides to the cytoplasmic membrane. The peptides were shown to associate with and enter into the membranes of liposomes with similar characteristics to anionic bacterial membranes using both charge:charge and hydrophobic interactions. Although the literature often suggests that most peptides work by perturbing membranes [1–3], it was quite clear here that, although RT2 and KT2 are able to interact with bacteria-like membranes, they have an extremely low ability to perturb such membranes and in fact in intact cells they are largely observed within the cells, indicating that interaction with the membrane does not lead per se to membrane damage. These peptides were designed to have both hydrophobic and positively designed domains in their sequence, so it is likely that their hydrophobic facets interact with the anionic lipid head groups (phosphatidyl glycerol and cardiolipin) at the surface of the cytoplasmic membrane of *E. coli* and insert into the hydrophobic core.

Our previous studies using circular dichroism suggested that in membrane-mimicking environments (LUV or SDS micelles), the secondary structure of peptides KT2 and RT2 was more ordered into α-helices (~30–40% α-helix content), which is lower than that recorded for magainin II and some other membrane-targeting peptides. It is possible that the shapes of these peptides upon interaction with bacterial membranes might be bent and this less ordered structure might favor translocation across the cytoplasmic membrane leading to DNA binding. The electrostatic interaction between polyanionic DNA and polycationic peptides enable the peptides to bind to DNA (and likely other nucleic acids) inside the bacterial cells which is observed as completely-filled bacterial cells (Fig. 6). Therefore, we propose that the mechanism of antibacterial action of peptides RT2 and KT2 is substantially based on their ability to bind to negatively-charged components of bacterial membranes (LPS and anionic phospholipids), translocate into bacterial cells (through peptide interactions with other peptide molecules and membrane phospholipids), and subsequently bind to intracellular polynucleotides to inhibit macromolecular synthesis.

Transparency document

The Transparency document associated with this article can be found, in the online version.

Acknowledgements

We would like to thank the Science Achievement Scholarship of Thailand (SAST), the National Research University Project of Thailand, Protein and Proteomics Research Center for Commercial and Industrial Purposes (ProCCI), and the Khon Kaen University for their financial assistance. REWH was funded by the Canadian Institutes of Health Research. REWH holds a Canada Research Chair in new antimicrobial discovery. CDLF-N received a scholarship from the Fundación "la Caixa" and Fundación Canadá (Spain). We also would like to thank Evan F. Haney for the dansyl-polymyxin synthesis.

References

[1] R.E.W. Hancock, H.G. Sahl, Antimicrobial and host-defence peptides as novel anti-infective therapeutic strategies, Nat. Biotechnol. 24 (2006) 1551–1557.
[2] C.D. Fjell, J.A. Hiss, R.E.W. Hancock, G. Schneider, Designing antimicrobial peptides: form follows function, Nat. Rev. Drug Discov. 11 (2012) 37–51.
[3] J.D. Hale, R.E.W. Hancock, The alternative mechanisms of action of cationic antimicrobial peptides on bacteria, Expert Rev. Anti Infect. Ther. 5 (2007) 951–959.
[4] M. Wenzel, A.I. Chiriac, A. Otto, D. Zweytick, C. May, C. Schumacher, R. Gust, H.B. Albada, M. Penkova, U. Krämer, R. Erdmann, N. Metzler-Nolte, S.K. Straus, E. Bremer, D. Becher, H. Brötz-Oesterhelt, H.G. Sahl, J.E. Bandow, Small cationic antimicrobial peptides delocalize peripheral membrane proteins, Proc. Natl. Acad. Sci. U. S. A. 111 (2014) 1409–1418.
[5] K. Matsuzaki, Magainins as paradigm for the mode of action of pore forming polypeptides, Biochim. Biophys. Acta 1376 (1998) 391–400.
[6] K. He, S.J. Ludtke, D.L. Worcester, H.W. Huang, Neutron scattering in the plane of membranes: structure of alamethicin pores, Biophys. J. 70 (1996) 2659–2666.
[7] M.P. Brennen, D. Cox, A.J. Chubb, Peptide diversity in drug discovery, Front. Drug Des. Discov. 3 (2007) 417.
[8] C.B. Park, H.S. Kim, S.C. Kim, Mechanism of action of the antimicrobial peptide buforin II: buforin II kills microorganisms by penetrating the cell membrane and inhibiting cellular functions, Biochem. Biophys. Res. Commun. 244 (1998) 253–257.
[9] H.G. Boman, B. Agerberth, A. Boman, Mechanisms of action on *Escherichia coli* of cecropin P1 and PR-39, two antibacterial peptides from pig intestine, Infect. Immun. 61 (1993) 2978–2984.
[10] T. Anunthawan, N. Yaraksa, S. Phosri, T. Theansungnoen, S. Daduang, A. Dhiravisit, S. Thammasirirak, Improving the antibacterial activity and selectivity of an ultra short peptide by hydrophobic and hydrophilic amino acid stretches, Bioorg. Med. Chem. Lett. 23 (2013) 4657–4662.
[11] L. Zhang, M.G. Scott, H. Yan, L.D. Mayer, R.E.W. Hancock, Interaction of polyphemusin I and structural analogs with bacterial membranes, lipopolysaccharide, and lipid monolayers, Biochemistry 39 (2000) 14504–14514.
[12] C. de la Fuente-Núñez, F. Reffuveille, E.F. Haney, S.K. Straus, R.E.W. Hancock, Broad-spectrum anti-biofilm peptide that targets a cellular stress response, PLoS Pathog. 10 (2014) 1004152.
[13] R.A. Moore, N.C. Bates, R.E.W. Hancock, Interaction of polycationic antibiotics with *Pseudomonas aeruginosa* lipopolysaccharide and lipid A studied by using dansyl-polymyxin, Antimicrob. Agents Chemother. 29 (1986) 496–500.
[14] R.F. Epand, M.A. Schmitt, S.H. Gellman, R.M. Epand, Role of membrane lipids in the mechanism of bacterial species selective toxicity by two α/β-antimicrobial peptides, Biochim. Biophys. Acta 1758 (2006) 1343–1350.
[15] M. Torrent, E. Cuyas, E. Carreras, S. Navarro, O. Lopez, A. de la Maza, M.V. Nogues, Y.K. Reshetnyak, E. Boix, Topography studies on the membrane interaction mechanism of the eosinophil cationic protein, Biochemistry 46 (2007) 720–733.
[16] G.R. Bartlett, Colorimetric assay methods for free and phosphorylated glyceric acids, J. Biol. Chem. 234 (1959) 469–471.
[17] D.J. Schibli, R.F. Epand, H.J. Vogel, R.M. Epand, Tryptophan-rich antimicrobial peptides: comparative properties and membrane interactions, Biochem. Cell Biol. 80 (2002) 667–677.
[18] D. Needham, E. Evans, Structure and mechanical properties of giant lipid (DMPC) vesicle bilayers from 20 degrees C below to 10 degrees C above the liquid crystal–crystalline phase transition at 24 degrees C, Biochemistry 27 (1988) 8261–8269.
[19] M. Torrent, D. Sánchez, V. Buzón, M.V. Nogués, J. Cladera, E. Boix, Comparison of the membrane interaction mechanism of two antimicrobial RNases:RNase 3/ECP and RNase 7, Biochim. Biophys. Acta 1788 (2009) 1116–1125.
[20] D.C. Morrison, D.M. Jacobs, Binding of polymyxin B to the lipid A portion of bacterial lipopolysaccharides, Immunochemistry 13 (1976) 813–818.
[21] L. Zhang, A. Rozek, R.E.W. Hancock, Interaction of cationic antimicrobial peptides with model membranes, J. Biol. Chem. 276 (2001) 35714–35722.
[22] H.T. Chou, H.W. Wen, T.Y. Kuo, C.C. Lin, W.J. Chen, Interaction of cationic antimicrobial peptides with phospholipid vesicles and their antibacterial activity, Peptides 31 (2010) 1811–1820.
[23] M. Magzoub, L.E. Eriksson, A. Gräslund, Comparison of the interaction, positioning, structure induction and membrane perturbation of cell-penetrating peptides and non-translocating variants with phospholipid vesicles, Biophys. Chem. 103 (2003) 271–288.
[24] A. Walrant, A. Vogel, I. Correia, O. Lequin, B.E. Olausson, B. Desbat, S. Sagan, I.D. Alves, Membrane interactions of two arginine-rich peptides with different cell internalization capacities, Biochim. Biophys. Acta 1818 (2012) 1755–1763.
[25] C. Bechara, S. Sagan, Cell-penetrating peptides: 20 years later, where do we stand? FEBS Lett. 587 (2013) 1693–1702.
[26] J.P. Powers, M.M. Martin, D.L. Goosney, R.E.W. Hancock, The antimicrobial peptide polyphemusin localizes to the cytoplasm of *Escherichia coli* following treatment, Antimicrob. Agents Chemother. 1522–1524 (2006).
[27] S.R. Schwarze, S.F. Dowdy, In vivo protein transduction: intracellular delivery of biologically active proteins, compounds and DNA, Trends Pharmacol. Sci. 21 (2000) 45–48.
[28] S.R. Schwarze, K.A. Hruska, S.F. Dowdy, Protein transduction: unrestricted delivery into all cells? Trends Cell Biol. 10 (2000) 290–295.
[29] M. Lindgren, M. Hällbrink, A. Prochiantz, Ü. Langel, Cell-penetrating peptides, Trends Pharmacol. Sci. 21 (2000) 99–103.
[30] J.S. Wadia, S.F. Dowdy, Protein transduction technology, Curr. Opin. Biotechnol. 13 (2002) 52–56.
[31] D.J. Mitchell, L. Steinman, D.T. Kim, C.G. Fathman, J.B. Rothbard, Polyarginine enters cells more efficiently than other polycationic homopolymers, J. Pept. Res. 56 (2000) 318–325.
[32] Y. Lan, Y. Ye, J. Kozlowska, J.K. Lam, A.F. Drake, A.J. Mason, Structural contributions to the intracellular targeting strategies of antimicrobial peptides, Biochim. Biophys. Acta 1798 (2010) 1934–1943.